RASĀYAN *J. Chem.*
Vol. 19 | No. 1 | 548-555 | January-March | 2026
ISSN: 0974-1496 | e-ISSN: 0976-0083 | CODEN: RJCABP
http://www.rasayanjournal.com
http://www.rasayanjournal.co.in

ADSORPTION ISOTHERM AND KINETIC STUDIES OF RHODAMINE B REMOVAL USING BIO WASTE-BASED ZIRCONIUM HYDROXYAPATITE ACTIVATED CARBONS

S. K. Reddy[1], R. U. Devi[2,✉], K. Hossain[3], and J. Swaraj[4]
[1]School of Science, GITAM Deemed (To Be) University, Vishakhapatnam-530045
[2]School of Science, GITAM Deemed (To Be) University, Hyderabad-502329
[3]Asutosh College, University of Calcutta, Kolkata-700073
[4]Environmental Protection Training and Research Institute (EPTRI), Hyderabad-500032
✉Corresponding author: urandhi@gitam.edu

ABSTRACT
This study examined the potential of activated carbons of Zirconium-Hydroxyapatite (Zr-HAP) produced from bio waste, that as fish bones, as an effective adsorbent material for the uptake of Rhodamine B, which is a xenobiotic dye. A hydrothermal method is used to synthesize fish bone waste-based Zr-HAP activated carbons. The characterisation of activated carbons' properties, specifically XRD, EDS, FTIR, SEM and TEM, was conducted. The adsorption efficiency of Rhodamine B correlates with the initial increase of Activated carbon dosage, reaching s saturation plateau at 40 ppm, with 100% removal observed at an optimal pH of 5 - 6. As the dye concentration increased, adsorption efficacy decreased, indicating monolayer adsorption at lower concentrations. Isotherm analysis suggested that the Langmuir model best described the process (with $R^2 = 0.969$), indicating homogenous adsorption. Kinetic modelling confirmed chemisorption with a pseudosecond-order mechanism being predominant. Thermodynamic analysis revealed the exothermic and spontaneous nature of the adsorption process. These study outcomes demonstrate that fish bone-based Zr-HAP activated carbon can be effectively utilised as an adsorbent for the removal of Rhodamine B in a sustainable process.
Key Words: Adsorption, Hydroxyapatite, Zirconium, Activated Carbons, Langmuir, and Kinetics
RASĀYAN*J. Chem.*, Vol. 19, No.1, 2025

INTRODUCTION

The excellent adsorption capacity of activated carbons (AC) over a wide variety of compounds, together with their low production cost, justifies their employment in the removal of various polluting agents from gaseous and liquid media.[1] Toxic heavy metal ions can be removed from aqueous solutions with activated carbon. In this case, adsorption occurs when metal ions form a surface complex with the acidic surface functional group of activated carbon. Hydroxyapatite [$Ca_{10}(PO_4)_6(OH)_2$] is an inorganic component of bone tissue; calcium/phosphate-based bioceramic is chemically comparable, non-inflammatory, non-immunogenic, biocompatible, and bioactive; and it can directly bond with live tissue. Zirconia-based composite materials have great corrosion resistance, high hardness, fracture toughness, and low magnetic susceptibility, making them beneficial for a wide range of biological applications.[2] AC, with its high specific surface area, typically demonstrates good removal efficiency for the majority of dissolved chemicals. It has a high ability for the adsorption of many organic compounds. Activated carbon is highly expensive, and its renewal generates extra effluent while resulting in a significant loss of adsorbent (10-15%). Over the years, waste materials from agricultural products such as rice straw, coconut husk, peat moss, etc., have been used as potential substitutes. At present, pollution from the textile industry is a severe environmental issue, and efficient purification has so far proven challenging. Because of carcinogenicity, reproductive and developmental toxicity, neurotoxicity, and chronic toxicity to people and animals, the Rhodamine B dye has been selected for the present study. The Rhodamine B ($C_{28}H_{31}N_2O_3Cl$) is a well-known fluorescent water tracer.[3] Thus, given the dangerous nature and detrimental impacts, it was deemed worthwhile to make systematic attempts to remove Rhodamine B from waste fluids utilising photochemical methods and adsorption over two adsorbents - activated carbon. This study used environmentally acceptable Zr-Hydroxyapatite (Zr-HAP) to develop a technique for

eliminating Rhodamine B from water pollutants.[4] In addition to cost, adsorptive qualities and availability are important considerations when selecting an adsorbent to remove contaminants.[5] This has fostered research into finding materials that are both efficient and inexpensive. Sawdust, slurry, biomass, cellulose, peat, chitin, chitosan, orange waste, rice husk, and wheat bran are examples of low-cost adsorbent materials employed by researchers. Furthermore, the results of the adsorption method by many investigators demonstrate the successful removal of heavy metals. This study focused on the adsorption of Rhodamine B from textile wastewater using fish bone-based Zr-HAP AC in an economic and eco-friendly approach.

EXPERIMENTAL

Boiling butcher bones for an hour defatted and deproteinized them. Washing removes impurities and soft tissues from bones. Pressing and sieving dry-cleaned bones into 45–125 micrometres. Zr-HAP is made by digesting 100 g of calcinated bone powder in Zirconium Chloride ($ZrOCl_2$) solution at pH 8 with 1M Ammonium Hydroxide for 5 hours. Calcium chloride, sodium hydroxide, potassium hydroxide, phosphoric acid, and 25% zinc chloride are added before carbonisation. Carbonising the source material at 450-900 CE follows. Carbonisation and chemical activation often occur together. Over physical activation, chemical activation is better due to lower temperatures and shorter duration. Mixing activated charcoal into the mixture (2:1) hydrothermally produced Zr-HAP nanoparticles. We vigorously stirred the suspension for three hours. After filtering and washing with deionised water and ethanol multiple times [7], these black Zr-HAP-AC nanoparticle precipitates were chemically analysed using FTIR, XRD, SEM, TEM, and EDAX. The pH, temperature, adsorbate concentration, adsorbent dose, and contact time were controlled in a batch mode Rhodamine-B adsorption test on Zr-HAP-ACs. Adsorption studies using 190–800 nm UV-visible spectrophotometers. The curve revealed the dye's best 550 nm adsorption. Absorbent dose (0.1 g–1 g), pH (1.0–12.0), contact time (5 min–120 min), dye concentration (5 ppm–100 ppm), and temperature (0 °C–100 °C) were considered adsorption parameters. The following investigations used ideal circumstances. After a certain period, the supernatant was collected and the quantity determined using spectrophotometry at the greatest MB/Rhodamine absorbance of 664 nm/514 nm (Eqn.-1).

$$q_e = \frac{Co-Ce}{m} * V \qquad (1)$$

The adsorbate removal efficiency (R%) from the solution is the metric used to evaluate adsorption (Eqn.-2).

$$R(\%) = \frac{Co-Ce}{Co} * 100 \qquad (2)$$

Research using the Freundlich adsorption isotherm model and the Langmuir adsorption isotherm model was carried out on activated carbons because of their potential as adsorbents for heavy metals and dyes (Eqn.-3 and 4)[8].

$$q = \frac{q_{max} K_L C}{1+K_L C} \qquad (3)$$

$$\frac{C_e}{q_e} = \frac{C_e}{q_m} + \frac{1}{bq_m} \qquad (4)$$

The non-linear Freundlich model is shown in Equation 5. Equation 6 delineates the linear Freundlich model.

$$q_e = K_F {C_n}^e \qquad (5)$$

$$log q_e = log K_F + \frac{log Ce}{n} \qquad (6)$$

RESULTS AND DISCUSSION

The crystal structure and microstructure orientation of the thin film sample AC-Zr-HAP was found with XRD by using the thin film detector and are depicted in Fig.-1. The XRD patterns clearly demonstrate the high crystallinity, and peaks corresponding to ZrO_2, HAP are seen. The diffraction peaks of the AC-Zr-HAP show the formation of the tetragonal phase of ZrO_2, and are matched well with the JCPDS card number 81-1455. The peaks obtained HAP at 2Θ values 26.0° (002), 32.2° (211), 36.0° (110), which corresponds to the hexagonal structure of hydroxy apatite and are well in accordance with that of JCPDS card number 09-0432.

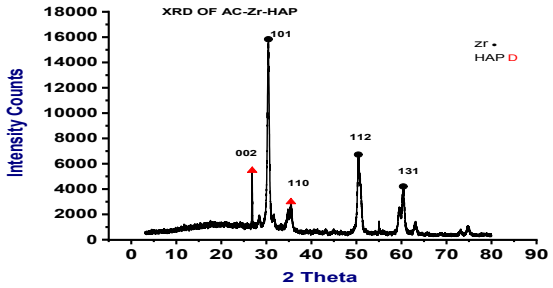

Fig.-1: XRD of AC-Zr-HAP

The films were distinctly homogeneous and demonstrated a notable dispersion of ZrO_2 components or the presence of ZrO_2 nanofibers embedded in HAP films. SEM images show that the film has a width of 7.7 µm to 7.8 µm (Fig.-2). The EDAX pattern and metal % at a specific location are displayed in Fig.-3. The functional groups of the composite film were identified by using FTIR spectroscopy and are shown in Fig.-3. The peaks corresponding to HAP were seen at 567cm^{-1}, 1055 cm^{-1}, and 1566 cm^{-1} (phosphate groups). The spectral data at the wave number values of 854, 1,413 and 1,451 cm^{-1} suggest the presence of carbonate ion. The characteristic peaks related to Zr-O stretching were seen at 466 and 434 were observed. All the peaks correspond to ZrO_2, and HAP are seen in the spectrum. TEM analysis showed AC-Zr-HAP shows the morphology, internal structure, particle size and arrangement in the low nanometer region (Fig.-4).

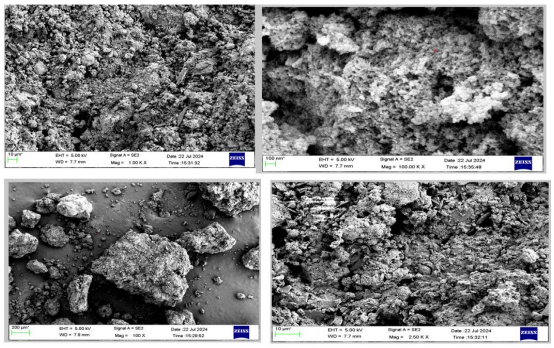

Fig.-2: SEM Images

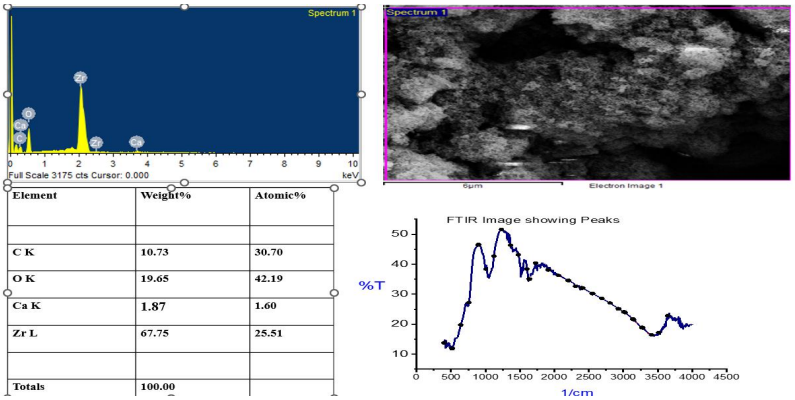

Element	Weight%	Atomic%
C K	10.73	30.70
O K	19.65	42.19
Ca K	1.87	1.60
Zr L	67.75	25.51
Totals	100.00	

Fig.-3: EDAX Pattern of Zr-CS-HAP and FTIR Image Showing Peaks

Changing the adsorbate dosage from 5 to 100 ppm examined the effect of initial Rhodamine B dye concentration on adsorption. To determine Rhodamine dye removal, the adsorbate was exposed for 40 min at pH 5 with varying amounts. Experimental results showed that dye removal increased with dye concentration, reaching 75.00% at 40 ppm. After that, the removal percentage dropped from 75.00% to 63.68% from 40 to 100 ppm. Exclusion efficacy increased because excess adsorbate (Rhodamine dye) adsorbed onto the adsorbent fast, resulting in maximal dye removal. Because dye molecules penetrated the adsorbent active sites at the saturation point, the percentage removal decreased with dye concentration.

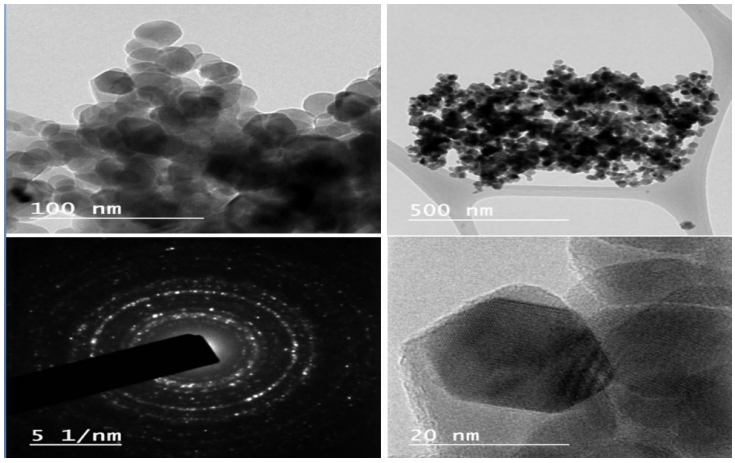

Fig.-4: TEM of AC-Zr-HAP

Adsorption Studies

Effect of pH and Temperature on Adsorption

The active group chemical state and surface charge distribution determine the target metal ion adsorbent affinity. Figure-6 shows how pH and adsorbent dosage affect water Rhodamine B dye removal. Negative adsorbent surface attracts positive ions, lowering solute equilibrium concentration when the solution pH rises to[9] at pH 5–6, 35.3% rhodamine B dye is removed. Dye removal improved till pH 6, then deteriorated. At low pH, the Adsorbents' negative charges are neutralised to improve protonation and dye adsorption. This increases diffusion and active sites on adsorbent surfaces, improving adsorption. Dye deproteination reduces dye concentration and transport when pH rises (Fig.-5).

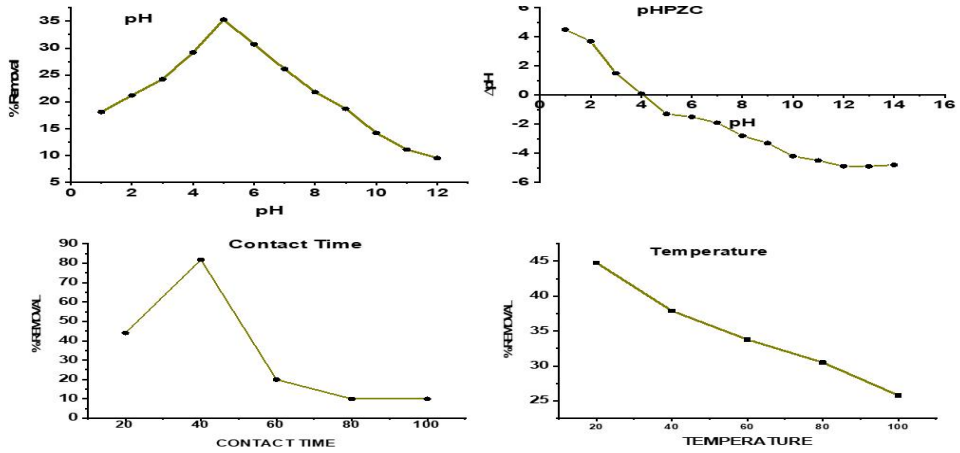

Fig.-5 pH Effect on Adsorption and Point of Zero Charge

At pH zero, adsorbents have no net electrical charge. These influences charged molecule-surface interactions in adsorption research. PZC depends on the adsorbent. The adsorbent's surface charge turns positive when the solution pH is below the PZC, allowing anions to be absorbed. When pH exceeds PZC, the surface charge is negative, permitting cation adsorption.[10] Increasing solution temperature decreases adsorption capability, according to experiments. This implies that metal ion adsorption on the adsorbent generates heat. Figure-6 shows metal ion elimination over contact time. Ion removal efficiency peaked at 40 minutes and did not improve from 40 to 100 minutes (Fig.-5). This may be because the solute concentration gradient was considerable and all adsorbent sites were empty at first. Research found that 40 minutes was ideal for interaction.[11]

Effect of Adsorbent Dosage

Under conditions of initial heavy metal concentrations ranging from 0.1 to 1.2 g/L, the impact of adsorbent dosage on heavy metal adsorption was investigated throughout a 180-minute contact time. With

an adsorbent dosage of 0.6 g, the highest heavy metal adsorption was achieved (Fig.-6). But after 0.6 g of dose, the percentage of heavy metals adsorbed did not vary significantly.

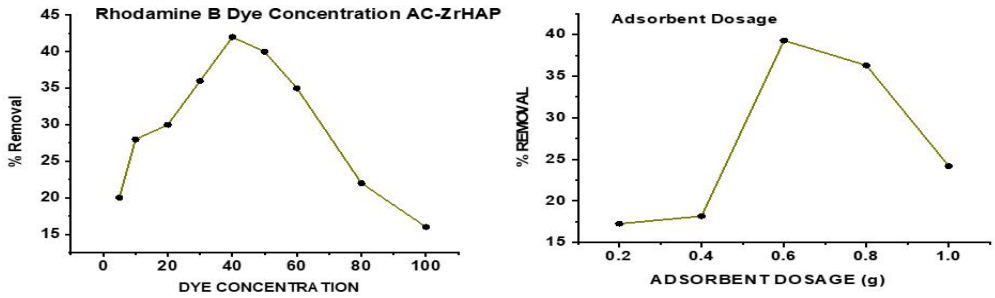

Fig.-6: Dye concentration and Adsorbent Dosage

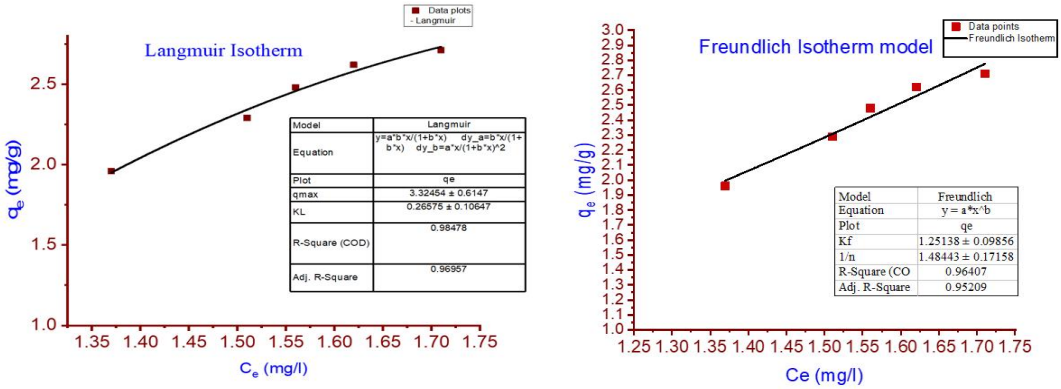

Fig.-7: Langmuir Isotherm and Freundlich Isotherm

At larger doses, the overlapping of active areas might be to blame. The accumulation of exchanger particles causes a reduction in the effective surface area. So, the optimal dose was thought to be 0.6 g.[12]

Adsorption Isotherm

The Langmuir and the Freundlich isotherms, as well as nonlinear curves, were used to analyse the adsorption data. Adsorption of Rhodamine B dye onto the surface of AC-Zr-HAP from an aqueous solution is depicted in Fig.-7 by means of the Langmuir Isotherm.

Table-1: Representing R^2 Values of Langmuir and the Freundlich Isotherm Values

Sample	Langmuir Isotherm				Freundlich Isotherm			
	1	2	3	4	1	2	3	4
	q max	K_L (Lmg^{-1})	R^2 COD	R^2 (Adjacent)	K_F(mgg^{-1}(Lmg^{-1})$^{1/n}$)	1/n	R^2 COD	R^2(Adjacent)
AC-Zr-HAP	3.32454 ± 0.6147	0.26575 ± 0.10647	0.98478	0.96957	1.25138 ± 0.09856	1.48443 ± 0.17158	0.96407	0.95209

The statistical data is consistent with the Langmuir isotherm model, as the R^2 value was 0.969, which is close to 1, and higher than the Freundlich isotherm value. The current adsorption process shows promise, as indicated by the R^2 value of 0.952 for the Freundlich isotherm model.

Adsorption Kinetics

At starting concentrations ranging from 5 to 40 mg/L, this study analysed the adsorption kinetics of Rhodamine B using pseudo-first-order, pseudo-second-order (Table-2).

$$q_t = q_e(1-\exp(-k_1 t)) \quad (7)$$

The equilibrium adsorption capacities (qe) increase from 1.00 mg/g at 5 mg/L to 16.80 mg/g at 40 mg/L as the starting concentration is increased. R^2 values between 0.948 and 0.960 indicate a good fit for the

kinetic models. At higher doses, the $q_e$values are often underestimated; for example, at 5 mg/L, they range from 1.05 mg/g to 18.15 mg/g. An R^2 value between 0.919 and 0.930 indicates a somewhat worse overall fit for the pseudo-second-order model. From 1.18 mg/g at 5 mg/L to 20.5 mg/g at 40 mg/L, it tends to overstate QE values at elevated doses. To add, K_2 values decrease with increasing concentrations, such as K2 0.0018 g/mg-min at 5 mg/L and 0.0003 g/mg-min at 40 mg/L (Fig.-8). In terms of accurately representing experimental q_e values, particularly at lower concentrations, the pseudo-first-order model outperforms the pseudo-second-order model when it comes to describing the adsorption dynamics of Rhodamine B removal using Zirconium hydroxyapatite activated carbons.[13]

Table-2: Adsorption Kinetic Parameters for Removing Rhodamine B

S. No.	Co(mg/L)	% Loss	qe(exp)(mg/g)	Pseudo First Order			Pseudo Second Order			Elovich Kinetics		
				qe(mg/g)	K_1(min^{-1})	R^2	qe(mg/g)	K_2(g/mg.min)	R^2	α	β	R^2
1	5	20	1.00	1.05	0.071	0.960	1.18	0.0018	0.930	0.011	3.20	0.850
2	10	28	2.80	3.00	0.064	0.958	3.36	0.0011	0.932	0.021	5.45	0.870
3	20	30	6.00	6.45	0.058	0.955	7.30	0.0008	0.928	0.028	8.90	0.875
4	30	36	10.80	11.65	0.051	0.952	13.1	0.0005	0.924	0.036	13.75	0.860
5	40	42	16.80	18.15	0.047	0.948	20.5	0.0003	0.919	0.043	18.80	0.858

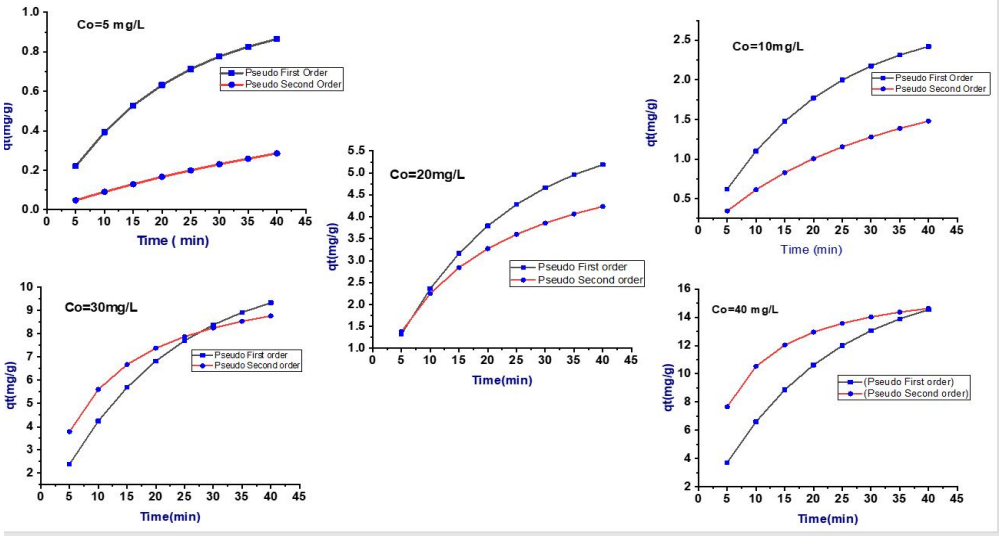

Fig.-8: Adsorption Kinetic Parameters for the Removal of Rhodamine B

Zirconium hydroxyapatite activated carbons adsorb Rhodamine B spontaneously and exothermically (Table-3). All concentrations show negative enthalpy change values (ΔH∘) ranging from -51.74 kJ/mol to -44.06 kJ/mol, indicating an exothermic adsorption process that releases heat. Negative entropy change (ΔS) values, ranging from -136.14 to -114.55 J/mol, suggest reduced randomness at the solid-liquid interface during adsorption. Gibbs free energy change (ΔG∘) values are negative at all temperatures (303 K to 333 K) and starting concentrations, indicating the spontaneous adsorption process. Rising temperatures decrease the spontaneity of the process, indicating an exothermic reaction, since (ΔG∘) values become less negative.

Table-3: Thermodynamic Parameters for the Removal of Rhodamine B

Concentration (mg/L)	% Loss	ΔH^0 (kJ/mol)	ΔS^0 (J/mol.K)	ΔG^o At 303 K (kJ/mol)	ΔG^o At 313 K (kJ/mol)	ΔG^o At 323 K (kJ/mol)	ΔG^o At 333 K (kJ/mol)
5	20	-51.74	-136.14	-10.49	-9.13	-7.77	-6.41
10	38	-50.59	-132.90	-10.32	-8.99	-7.67	-6.34
20	30	-48.35	-126.58	-9.99	-8.73	-7.46	-6.19
30	36	-46.17	-120.46	-9.67	-8.46	-7.26	-6.05
40	42	-44.06	-114.55	-9.35	-8.21	-7.06	-5.91

Higher concentrations (e.g., 40 mg/l) exhibit lower spontaneity (ΔG∘) at 303 K = -9.35 kJ/mol, while lower concentrations (5 mg/l) have stronger spontaneity (ΔG^0) at -10.49 kJ/ As temperature rises, ΔG decreases, indicating more adsorption,[14] discovered that greater temperatures lead to better Orange G dye adsorption, indicating an exothermic process with lower ΔG values. BG 4 and AF adsorption on activated carbon is exothermic and spontaneous, reducing ΔG values with rising temperature.[15] The negative value of ΔG is caused by rising temperature, which raises ΔS. ΔG is inversely related to ΔH. High dye concentration and temperature reduce adsorption. Adsorption is thermodynamically beneficial, but concentration and temperature impact it. Negative ΔH^0 values at all concentrations indicate an exothermic adsorption mechanism. Adsorption is spontaneous, as shown by consistently negative ΔG^0 values at all temperatures (303 K to 333 K). Negative ΔS^0 values suggest less unpredictable adsorption at the solid-liquid interface. As dye concentration rises, ΔH^0, ΔS^0, and ΔG^0 decrease, indicating reduced adsorption favorability. This suggests dye concentration saturates adsorption sites, making the process less energy-efficient.

CONCLUSION

Metal ions, hydroxyl apatite (HAP), and activated charcoal form a very effective composite material with biocompatibility, adsorption efficiency, and environmental applications. The composite material uses activated charcoal's porosity and surface area, hydroxyl apatite's ion exchange and bioactivity, and doped metal ions' catalytic or adsorption-enhancing properties. XRD, FTIR, EDAX, SEM, and TEM have revealed the composite's structure, surface chemistry, and morphology before and after dye adsorption. FTIR study showed that dye molecules interact with hydroxyl and carbonyl functional groups in adsorption. SEM pictures showed Rhodamine B molecules covering and filling pores following adsorption. A best fit with the Langmuir model (R^2=0.969) indicates monolayer adsorption on a homogenous surface with finite adsorption sites in isotherm modelling. Kinetic analysis further showed that the adsorption followed a pseudo-second-order model, implying chemisorption. For Rhodamine B adsorption from water systems, fishbone-derived Zr-HAP activated carbon is cost-efficient, environmentally benign, and effective. High adsorption capacity, versatility to varied adsorption models, and promising kinetic and thermodynamic features make this adsorbent a good bet for future practical applications.

ACKNOWLEDGMENTS

The authors are grateful to GITAM Deemed to Be University, Hyderabad.

AUTHOR CONTRIBUTIONS

The present work is related to *SDG-6:Clean water and Sanitation*. All the authors contributed significantly to this manuscript, participated in reviewing/editing and approved the final draft for publication. The research profile of the authors can be verified from their ORCID ids, given below:

Sumila Kunduru https://orcid.org/0009-0003-4815-6880
Randhi Uma Devi https://orcid.org/0000-0002-3240-3248
Kaizar Hossain https://orcid.org/0000-0002-3903-6161
J.Swaraj https://orcid.org/0000-0001-9458-4526

Cite this article as: S. K. Reddy *et al.*, *Rasayan J. Chem.*, 19(1), 548-555(2026), https://doi.org/10.31788/RJC.2026.1919528.

REFERENCES

1. Z. Heidarinejad, M.H. Dehghani, M. Heidari, G. Javedan, I. Ali and M. Sillanpaa, *Environmental Chemistry Letters*, **18**(2), 393(2020), https://doi.org/10.1007/s10311-019-00955-0
2. C.R.D. Ferreira, A.A.G. Santiago, R.C. Vasconcelos, D.F.F. Paiva, F.Q. Pirih, A.A. Araújo, F.V. Motta and M.R.D. Bomio, *Ceramics International*, **48**(9), 12376(2022), https://doi.org/10.1016/j.ceramint.2022.01.102

3. M. Oplatowska-Stachowiak and C.T. Elliott, *Critical Reviews in Food Science and Nutrition*, **57**(3), 524(2017), https://doi.org/10.1080/10408398.2014.889652
4. G.A.A. Al-Hazmi, A.A. El-Zahhar, M.G. El-Desouky, M.A. El-Bindary and A.A. El-Bindary, *Journal of Coordination Chemistry*, **75**(9–10), 1203(2022), https://doi.org/10.1080/00958972.2022.2114349
5. T.S. Vo, M.M. Hossain, H.M. Jeong and K. Kim, *Nano Convergence*, **7**, 25(2020), https://doi.org/10.1186/s40580-020-00245-4
6. W.S. Wan Ngah and M.A.K.M. Hanafiah, *Biochemical Engineering Journal*, **39**(3), 521(2008), https://doi.org/10.1016/j.bej.2007.11.006
7. R. Mogale, K.G. Akpomie, J. Conradie and E.H.G. Langner, *Journal of Environmental Management*, **304**, 114166(2022), https://doi.org/10.1016/j.jenvman.2021.114166
8. W. Shen, S. Chen, S. Shi, X. Li, X. Zhang, W. Hu and H. Wang, *Carbohydrate Polymers*, **75**(1), 110(2009), https://doi.org/10.1016/j.carbpol.2008.07.006
9. B. Wang, J. Lan, C. Bo, B. Gong and J. Ou, *RSC Advances*, **13**(7), 4380(2023), https://doi.org/10.1039/d2ra07911a
10. K. Jedynak and B. Charmas, *Materials*, **14**(14), 3859(2021), https://doi.org/10.3390/ma14143859
11. A. Bazan-Wozniak, A. Jędrzejczak, R. Wolski, S. Kaczmarek, A. Nosal-Wiercińska, J. Cielecka-Piontek, S. Yagmur-Kabas and R. Pietrzak, *Molecules*, **29**(6), 1412(2024), https://doi.org/10.3390/molecules29061412
12. A. Rahmani, H.Z. Mousavi and M. Fazli, *Desalination*, **253**(1–3), 94(2010), https://doi.org/10.1016/j.desal.2009.11.027
13. M. Manjuladevi, R. Anitha and S. Manonmani, *Applied Water Science*, **8**, 36(2018), https://doi.org/10.1007/s13201-018-0674-1
14. R. Gopinathan, A. Bhowal and C. Garlapati, *Journal of Chemical and Engineering Data*, **62**(1), 398(2017), https://doi.org/10.1021/acs.jced.6b00845
15. J. Sheeja, K. Sampath and R. Kesavasamy, *Adsorption Science & Technology*, **2021**, 5035539(2021), https://doi.org/10.1155/2021/5035539

[RJC-9528/2025]